Effects of Foreign Gases on Dual Fluorescences of Pyrene Vapor

Kohji CHIHARA and Hiroaki BABA

Division of Chemistry, Research Institute of Applied Electricity, Hokkaido University, Sapporo 060

(Received July 29, 1975)

The characteristics of the dual fluorescences of pyrene vapor at 170 °C and 0.2—0.3 Torr have been investigated in the presence of cyclohexane or oxygen. With increasing cyclohexane pressure, the S_1-fluorescence shows a blue shift and an increase in quantum yield and in lifetime, while the S_2-fluorescence shows only a slight blue shift and a marked decrease in yield and in lifetime. Oxygen efficiently quenches the S_1- and S_2-fluorescence according to the Stern-Volmer relation. The experimental results are well explained by kinetic analyses based on the following assumptions: (1) The internal conversion is reversible and is much faster than other radiative and radiationless processes; (2) cyclohexane causes only vibrational relaxation which can be described in terms of a simple stepladder model; (3) oxygen acts as a quencher on both S_1- and S_2-fluorescence emissions. It is found that one collision with cyclohexane removes on the average a vibrational energy of the order of 1000 cm^{-1} or less from S_1 or S_2 of pyrene, and that one collision with oxygen quenches S_1 or S_2 with a probability close to unity. It is concluded that the S_2-fluorescence consists mainly of a slow component originating from S_2 which is in equilibrium with S_1.

In relation to the theories of radiationless transitions in isolated molecules,[1,2] a number of experimental studies[3,4] have recently been made of the emission properties of organic compounds in the vapor phase at low pressure, where molecules are free from collision during their emission lifetimes. Under such conditions the fluorescence of organic molecules presents peculiar features that cannot be seen in a condensed phase or in a vapor at a high pressure. Thus, in the low-pressure vapor, pyrene and related compounds are known to exhibit distinct fluorescence emission from the second excited singlet (S_2) in addition to the ordinary fluorescence from the first excited singlet (S_1).[5-9]

In previous papers,[5,6] hereafter referred to as Papers I and II respectively, the following observations were reported on the dual fluorescences of pyrene and its simple derivatives in the vapor phase. (1) As the excitation energy increases, the S_2-fluorescence shifts to the red in much the same way as the S_1-fluorescence, and both S_1- and S_2-fluorescence bands become broad. (2) The quantum yield of the S_2-fluorescence (Φ_{2F}) increases rapidly with excitation into successively higher singlet states, whereas the yield of the S_1-fluorescence (Φ_{1F}) decreases only slowly with increasing excitation energy. The ratio Φ_{2F}/Φ_{1F} is roughly related to ρ_2/ρ_1, where ρ_1 and ρ_2 are the densities of vibrational states in S_1 and S_2 at the energy of excitation. (3) Addition of cyclohexane as an inert foreign gas to the pyrene vapor results in a marked decrease in Φ_{2F}/Φ_{1F}. (4) Most of the S_2-fluorescence emission seems to occur through the mechanism involving reverse internal conversion.

In the presence of cyclohexane, pyrene must undergo vibrational relaxation in its excited state. On the other hand, the excited singlet state of many aromatic compounds including pyrene is known to be quenched by oxygen very efficiently.[10,11] It is to be expected that the changes in emission characteristics caused by addition of such foreign gases are different between the S_1- and S_2-states of pyrene vapor.

The purpose of the present study is to gain a deeper insight into the nature of the dual fluorescences through a detailed examination of the effects of foreign gases, cyclohexane and oxygen, on the S_1- and S_2-emissions of the pyrene molecule in the vapor phase.

Experimental

Pyrene and cyclohexane were purified in the same way as in Paper I. Oxygen obtained from Takachiho Kagaku Kogyo Co. (purity, 99.8%) was used as received. The methods for preparation of the sample vapor, measurement and correction of fluorescence spectra, and for determination of fluorescence quantum yields were the same as described in Paper I, unless otherwise stated. All the experiments were conducted at 170 °C and at pyrene pressures in the range 0.2—0.3 Torr.

Measurements of fluorescence emission of low intensity were made on a high-sensitivity emission spectrophotometer constructed recently in our laboratory. In this spectrophotometer, light from a 150-W xenon lamp was dispersed by a Czerny-Turner double monochromator with an f number of 4.5, consisting of a quartz prism and a grating (1200 lines/mm), to give monochromatic excitation beam. The fluorescence emitted from the sample at right angles to the excitation beam was dispersed by another Czerny-Turner monochromator with an f number of 4.5, consisting of a 1200 lines/mm grating alone. The resulting monochromatic fluorescence emission was detected by the photon counting method, using a Hamamatsu R585 photomultiplier which showed at room temperature a very low dark current corresponding to ~1 count/s. Both excitation and emission wavelengths were scanned discontinuously with the aid of a pulse motor. Fluorescence with a quantum yield as low as 10^{-7} can be measured with this spectrophotometer, provided that an optimum concentration of sample material is used. For fluorescence of higher intensity another emission spectrophotometer was used which was constructed by attaching a photon counting system, similar to the one mentioned above, to the optical system of a Hitachi MPE-2A fluorescence spectrophotometer.

The fluorescence decay was observed using a breakdown spark generated in 2-atm oxygen gas as the exciting light source. The breakdown was induced by a Japan Electron Optics Laboratory JLS-R3A giant pulse ruby laser with a peak output of 150 MW. The oxygen breakdown spark has a high intensity and a duration of about 70 ns, and covers the necessary wavelength range of 210—330 nm. The light beam from the breakdown spark was passed through the following filter systems (a) and (b) for exciting the pyrene molecule into its S_3- and S_4-states, respectively; (a) consists of an interference filter with a transmittance maximum of 17.5% at 264.5 nm and a half bandwidth of 14 nm and a solution filter obtained by dissolving 1.1 mg of 2,7-dimethyl-

3,6-diazacyclohepta-1,6-diene perchlorate in 25 ml water, and (b) is an interference filter with a transmittance maximum of 19% at 234 nm and a half bandwidth of 23 nm. Note that the solution filter in (a) cuts off the stray light falling into the wavelength region of S_2-fluorescence. A monochromator was used for selecting the emission wavelength. For the measurement of S_1-fluorescence decay in the absence of a foreign gas, excitation was made at each of the vibrational peaks belonging to individual electronic absorption bands. In this case, a monochromator was used for selecting the wavelength of the exciting light of the breakdown spark, with the bandwidth being set to 8 nm, and the emission beam was passed through filters of UV-D2 and UV-35 from Toshiba Electric Co., which excluded the scattered exciting light and the S_2-fluorescence emission. All the fluorescence lifetimes were determined by the deconvolution method.[12]

Results

The excited singlet states associated with the four electronic absorption transitions of pyrene appearing in the near ultraviolet region (Paper I) are denoted by $S_1, \cdots, S_4$ in order of increasing energy, and the ground singlet state by S_0. The zero vibrational level of each of the electronic states will be represented by a superscript 0, *e.g.*, S_2^0. The $S_0 \rightarrow S_2, \rightarrow S_3$, and $\rightarrow S_4$ transitions show a prominent progression in a totally symmetric carbon stretching vibration of 1400 cm^{-1} frequency (*cf.* Papers I and II). The vibrational levels related to this progression will be expressed as S_2^v *etc.*, where v refers to the quantum number of the vibration concerned (v=0, 1, 2, ···).

The effects of cyclohexane added as an inert foreign gas on the S_1- and S_2-fluorescence were examined by exciting the pyrene molecule into various vibronic levels. As an example, changes in fluorescence spectrum caused by addition of different pressures of cyclohexane are shown in Fig. 1 for excitation into S_4^0. Similar spectral

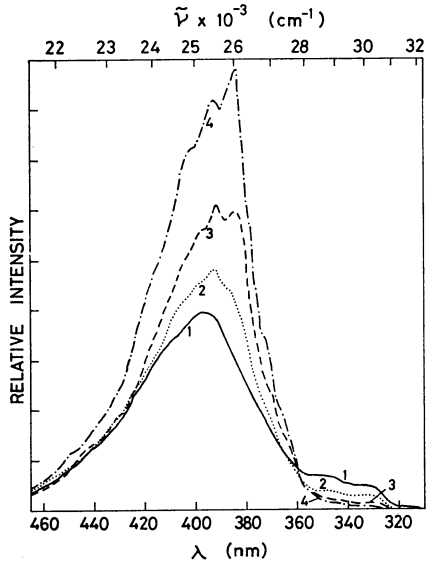

Fig. 1. Fluorescence spectra of pyrene vapor excited at 234 nm (S_4^0) in the presence of cyclohexane of different pressures: (1) 0; (2) 6.3; (3) 23.4; (4) 47.5 Torr. The relative intensity means relative quanta per unit wave-number interval.

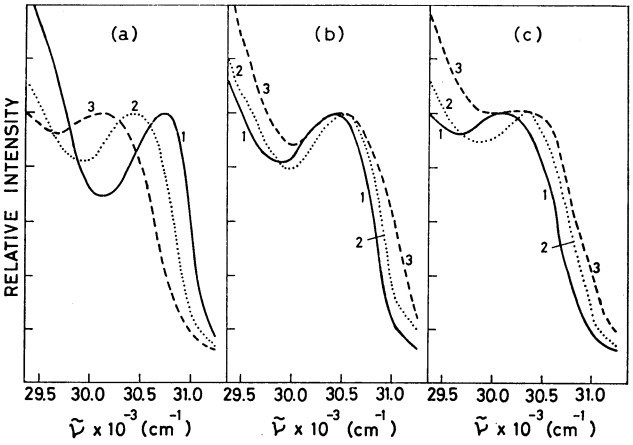

Fig. 2. S_2-fluorescence spectra (normalized) of pyrene vapor. (a) Excited in the absence of cyclohexane at different wavelengths: (1) 298 nm (S_2^2); (2) 266 nm (S_3^0); (3) 234 nm (S_4^0). (b) Excited at 266 nm (S_3^0) in the presence of cyclohexane of different pressures: (1) 0; (2) 12.5; (3) 164 Torr. (c) Excited at 234 nm (S_4^0) in the presence of cyclohexane of different pressures: (1) 0; (2) 23.4; (3) 164 Torr. The relative intensity as in Fig. 1.

changes were observed for excitation into other vibronic levels. As is seen from Fig. 1, cyclohexane has considerable effects on the fluorescence spectra both in position and in intensity. With increasing cyclohexane pressure, the S_1-fluorescence shows a blue shift and an increase in intensity, while the S_2-fluorescence shows only a slight blue shift and a marked decrease in intensity.

The blue shift of the S_1-fluorescence spectrum is clearly seen in Fig. 1. The spectral shifts of the S_2-fluorescence due to the added cyclohexane are illustrated in Fig. 2 for excitation into S_3^0 and S_4^0, together with the frequency shift that occurs on changing the excitation energy in the absence of cyclohexane, *i.e.*, in the pure pyrene vapor. The quantum yields of S_1- and S_2-fluorescence are plotted against the cyclohexane

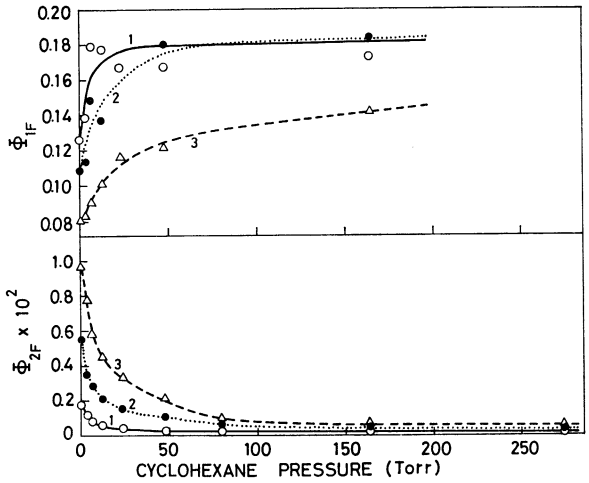

Fig. 3. Plots of Φ_{1F} and Φ_{2F} for pyrene vapor *vs.* the pressure of cyclohexane. Exciting wavelengths: (1) 298 nm (S_2^2); (2) 266 nm (S_3^0); (3) 234 nm (S_4^0).

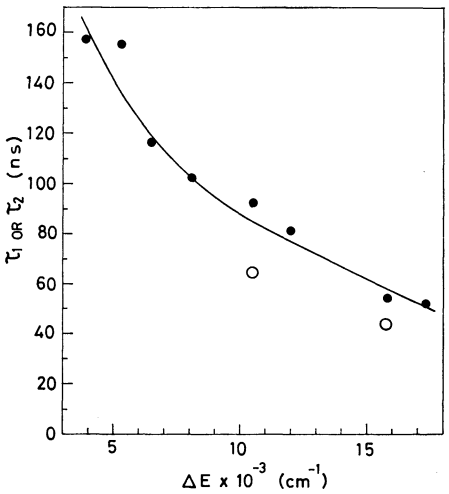

Fig. 4. Plots of τ_1 (●) and τ_2 (○) for pyrene vapor *vs.* ΔE.

pressure in Fig. 3 for excitation into different vibronic levels.

The lifetimes of the S_1- and S_2-fluorescence in the absence of cyclohexane, τ_1 and τ_2, are plotted in Fig. 4 against ΔE, which represents the excitation energy in excess of the $S_0^0 \rightarrow S_1^0$ transition energy. Both τ_1 and τ_2 are found to decrease with increasing ΔE. In the presence of cyclohexane, vibrational relaxation must occur in each of the excited electronic states, so that the molecules are distributed among various vibrational levels. The apparent lifetimes obtained in such a condition will be denoted by $\bar{\tau}_1$ and $\bar{\tau}_2$ (instead of τ_1 and τ_2) for S_1- and S_2-fluorescence, respectively. Figure 5 shows $\bar{\tau}_1$ and $\bar{\tau}_2$ as a function of the cyclohexane pressure. It is seen that the lifetime $\bar{\tau}_1$ increases but $\bar{\tau}_2$ decreases with the inert gas pressure, irrespective of excitation energy.

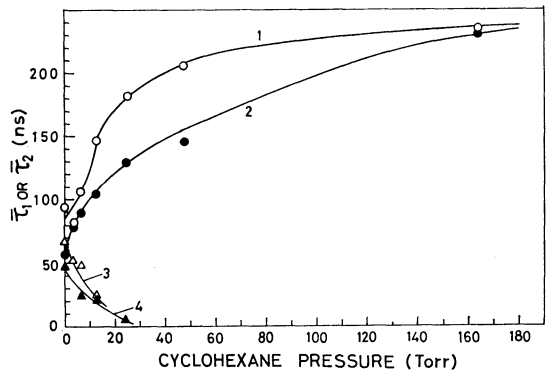

Fig. 5. Plots of $\bar{\tau}_1$ (1, 2) and $\bar{\tau}_2$ (3, 4) for pyrene vapor *vs.* the pressure of cyclohexane. Exciting and monitoring wavelengths: (1) 264.5 nm ($\sim S_3^0$), 400 nm (S_1); (2) 234 nm (S_4^0), 400 nm (S_1); (3) 264.5 nm ($\sim S_3^0$), 330 nm (S_2); (4) 234 nm (S_4^0), 330 nm (S_2).

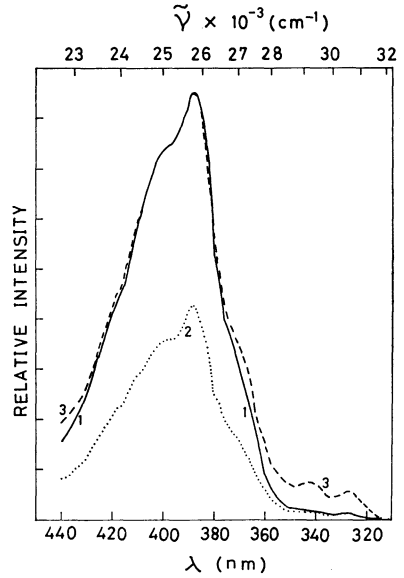

Fig. 6. Fluorescence spectra of pyrene vapor excited at 298 nm (S_2^2) in the presence of oxygen of different pressures: (1) 0; (2) 10.2; (3) 350 Torr. The relative intensity as in Fig. 1. The maximum intensities of spectra 1 and 3 are normalized to a common value (I_{max}); the maximum intensity of spectrum 2 is normalized to $I_{max}/2$.

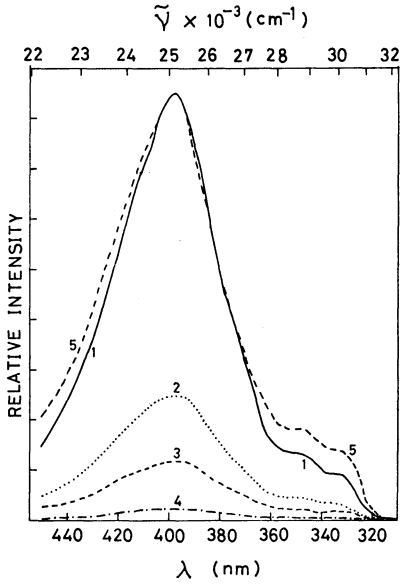

Fig. 7. Fluorescence spectra of pyrene vapor excited at 234 nm (S_4^0) in the presence of oxygen of different pressures: (1) 0; (2) 6; (3) 15; (4) 102; (5) 350 Torr. The relative intensity as in Fig. 1. The intensities of spectra 1—4 are given according to the respective observed emission signals; the maximum intensity of spectrum 5 is normalized to that of spectrum 1.

The effects of added oxygen on the fluorescence properties of pyrene vapor are quite different from the effects of cyclohexane. The spectral changes accompanying the addition of various pressures of oxygen are shown in Figs. 6 and 7, respectively, for S_2^2 and S_4^0 excitation. It is seen that in contrast to the case of cyclohexane oxygen acts as a quencher on both S_1- and S_2-fluorescences, and that the quantum yield ratio Φ_{2F}/Φ_{1F} increases, though slightly, with increasing oxygen pressure.

In Fig. 8 Φ_{1F}^0/Φ_{1F} and Φ_{2F}^0/Φ_{2F} are plotted against the oxygen pressure for S_2^2, S_3^0, and S_4^0 excitation; here, the fluorescence quantum yields in the absence and presence of oxygen are denoted by Φ_{1F}^0 (or Φ_{2F}^0) and Φ_{1F} (or Φ_{2F}),

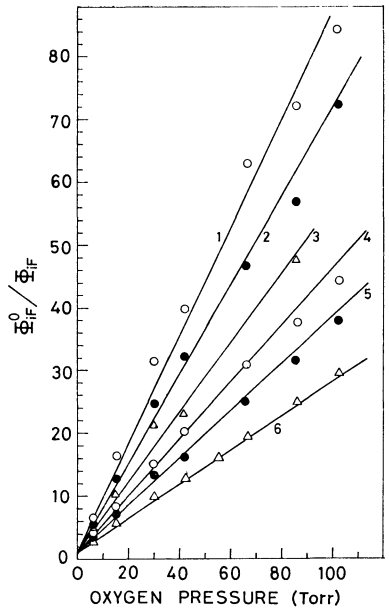

Fig. 8. Stern-Volmer plots for quenching of S_1-fluorescence (1, 2, 5) and S_2-fluorescence (3, 4, 6) of pyrene vapor by oxygen. Exciting wavelengths: (1) 298 nm (S_2^2); (2) 266 nm (S_3^0); (3) 298 nm (S_2^2); (4) 266 nm (S_3^0); (5) 234 nm (S_4^0); (6) 234 nm (S_4^0). For Φ_{iF}^0/Φ_{iF}, $i=1$ or 2.

respectively. The plots are found to be linear over a wide range of the quantum yield ratio, Φ_{1F}^0/Φ_{1F} or Φ_{2F}^0/Φ_{2F}, indicating that the Stern-Volmer equation holds in every case.

Discussion

As has been mentioned, the present experiments were made with the pyrene vapor at 0.2—0.3 Torr and 170 °C. Under these conditions, the mean time between collisions of pyrene molecules (*cf.* Paper I) is somewhat longer than the observed fluorescence lifetimes τ_1 and τ_2 (Fig. 4). It is assumed here, to the first approximation, that the pyrene molecule in the absence of a foreign gas is free from collisions in its excited state S_1 or S_2.

Intramolecular radiative and radiationless processes in polyatomic molecules can be treated both quantum-mechanically and kinetically.[2] In the following, the effects of foreign gases on the dual fluorescences of pyrene vapor will be discussed on the basis of a kinetic scheme involving reverse internal conversion, as in the case of Paper I.

For the pure pyrene vapor, the above scheme predicts that most of the S_2-fluorescence emission should occur through the reverse internal conversion, with its lifetime (τ_2) equal to that of the S_1-fluorescence (τ_1). The S_2-emission of this sort may be called slow S_2-fluorescence, because the lifetime τ_2 is very long compared not only with the lifetime of the direct or prompt S_2-fluorescence but also with the radiative lifetime of S_2 which is to be determined from the integrated absorption intensity. The experiments on the fluorescence quenching by oxygen clearly indicate that the S_2-emission is ascribable almost exclusively to the slow S_2-fluorescence. Also, the lifetime measurements show that τ_2 is comparable, though not strictly equal, to τ_1 in length.

In the absence of a foreign gas, the kinetic analysis given in Paper I is applicable. It is thus assumed that an isolated pyrene molecule is excited directly or indirectly to S_2*, *i.e.* a vibrationally excited level of S_2, and then passes to S_1* whose energy $E(S_1^*)$ is equal to the energy of S_2*, $E(S_2^*)$. It is further assumed that the molecule may return to S_2* from S_1*.

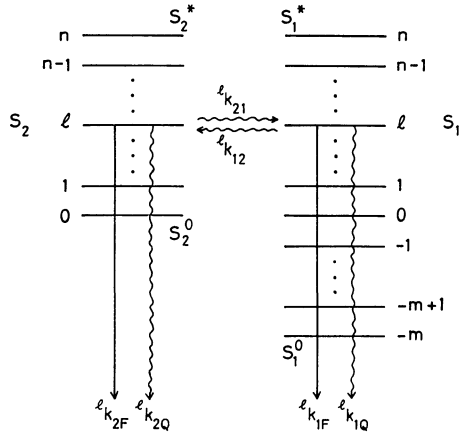

Fig. 9. A schematic diagram showing a stepladder model for vibrational relaxation in S_1- and S_2-states together with various electronic processes involved. Straight-line arrows denote radiative processes, and wiggly-line arrows radiationless processes.

Effects of Cyclohexane. In order to have an understanding of the effects of an inert foreign gas X, *i.e.* cyclohexane in this study, on the emission properties of pyrene vapor, we consider a simple stepladder relaxation model[13] illustrated in Fig. 9. We assume that only a finite series of vibrational levels, represented by $l=n, n-1, \cdots, 0$ for S_2 and by $l=n, \cdots, 0, \cdots, -m$ for S_1, participates in the collision-induced vibrational relaxation, with n, 0, and $-m$ corresponding to S_2* (or S_1*), S_2^0, and S_1^0, respectively. For $n \geqq l \geqq 0$, the vibrational levels $l(S_2)$ and $l(S_1)$ in the stepladder model are isoenergetic with each other, and reversible internal conversion is supposed to occur between them. The difference in energy between any two adjacent levels with $l \geqq 0$ or $l \leqq 0$ is equated to the amount of energy $\triangle\varepsilon$ or $\triangle\varepsilon'$ removed on the average by one collision between a pyrene and an X molecule. Thus we have simple relations $[E(S_2^*)-E(S_2^0)]/\triangle\varepsilon=n$ and $[E(S_2^0)-E(S_1^0)]/\triangle\varepsilon'=m$, where $\triangle\varepsilon'$ may or may not be equal to $\triangle\varepsilon$. Various rate constants for radiative and radiationless processes are defined in Fig. 9.

If the concentration of pyrene in a vibrational level $l(S_i)$ ($i=1$ or 2) in the stepladder model is expressed as $[l]_i$, the following general rate equations are obtained by reference to Fig. 9:

$$\frac{d[l]_2}{dt} = k_C[X][l+1]_2 + {}^{l}k_{12}[l]_1 - {}^{l}\lambda_2[l]_2 \quad (1)$$

$$\frac{d[l]_1}{dt} = k_C[X][l+1]_1 + {}^{l}k_{21}[l]_2 - {}^{l}\lambda_2[l]_1 \quad (2)$$

where

$${}^{l}\lambda_2 = {}^{l}k_{2F} + {}^{l}k_{2Q} + {}^{l}k_{21} + k_C[X] \quad (3)$$

$$ {}^{l}\lambda_1 = {}^{l}k_{1F} + {}^{l}k_{1Q} + {}^{l}k_{12} + k_C[X] \quad (4) $$

k_C is the bimolecular rate constant for the vibrational relaxation by collision and [X] is the concentration of the inert gas X; namely, $k_C[X]$ is the frequency of collision of a pyrene molecule with X molecules. Equations (1) and (3) apply to $n \geqq l \geqq 0$, and (2) and (4) to $n \geqq l \geqq -m$. However, for $l=n$, $[l+1]_i$ in Eqs. (1) and (2) is taken as equal to zero; for $l=0$ and $-m$, the term $k_C[X]$ is removed from Eqs. (3) and (4), respectively; and for $-1 \geqq l \geqq -m$, ${}^{l}k_{21}[l]_2$ in Eq. (2) and ${}^{l}k_{12}$ in Eq. (4) are eliminated. Further, in the case of steady photo-excitation, the rate of excitation (I_0) should be added to the right-hand side of Eq. (1) for $l=n$.

As will be shown later, the following relations exist among the rate constants for the pyrene molecule:

$$ {}^{l}k_{21} \gg {}^{l}k_{2F} + {}^{l}k_{2Q} \quad (5) $$

$$ {}^{l}k_{12} \gg {}^{l}k_{1F} + {}^{l}k_{1Q} \quad (6) $$

$$ {}^{l}k_{21} \gg {}^{l}k_{12} \quad (7) $$

Although the term $k_C[X]$ increases with the inert gas pressure, we have

$$ {}^{l}k_{21} \gg k_C[X] \quad (8) $$

$$ {}^{l}k_{12} \gg k_C[X] \text{ or } {}^{l}k_{12} \gtrsim k_C[X] \quad (9) $$

under the present experimental conditions.

Let us first consider the case of steady excitation. Under photostationary conditions $d[l]_i/dt=0$ in Eqs. (1) and (2). When $l=n$, it follows from Eq. (2) and inequality (6) that

$$ [n]_1/[n]_2 = {}^{n}k_{21}/({}^{n}k_{12}+k_C[X]) \quad (10) $$

Using inequalities (5)—(9), we can verify from Eqs. (1) and (2) that

$$ [l]_1/[l]_2 = {}^{l}k_{21}/{}^{l}k_{12} \quad (n-1 \geqq l \geqq 0) \quad (11) $$

It is useful to define a sort of equilibrium constant ${}^{l}K$ and an effective rate constant ${}^{l}k_{\text{eff}}$ for $n \geqq l \geqq 0$ by

$$ {}^{l}K = {}^{l}k_{21}/{}^{l}k_{12} \quad (12) $$

$$ {}^{l}k_{\text{eff}} = ({}^{l}k_2 + {}^{l}K\,{}^{l}k_1)/(1+{}^{l}K) \quad (13) $$

where

$$ {}^{l}k_i = {}^{l}k_{iF} + {}^{l}k_{iQ} \quad (i=1 \text{ or } 2) \quad (14) $$

Also, for $n \geqq l \geqq 0$, we put

$$ [l]_1 + [l]_2 \equiv [l] \quad (15) $$

We can then derive the following equations:

$$ [n] = I_0/({}^{n}k_{\text{eff}}+k_C[X]) \quad (16) $$

$$ [l-1] = [l]\frac{k_C[X]}{{}^{l-1}k_{\text{eff}}+k_C[X]} \quad (n \geqq l \geqq 1) \quad (17) $$

$$ [l-1]_1 = [l]_1\frac{k_C[X]}{{}^{l-1}k_1+k_C[X]} \quad (0 \geqq l \geqq -m+2) \quad (18) $$

$$ [-m]_1 = [-m+1]_1 k_C[X]/{}^{-m}k_1 \quad (19) $$

Combining inequalities (7) and (8) with Eqs. (10)—(12), we obtain the relations $[l]_2 \ll [l]_1$ and ${}^{l}K \gg 1$ for $n \geqq l \geqq 0$. Hence

$$ [l]_1 \simeq [l] \quad (n \geqq l \geqq 0) \quad (20) $$

$$ [n]_2 \simeq [n]\frac{1+k_C[X]/{}^{n}k_{12}}{{}^{n}K} \quad (21) $$

$$ [l]_2 \simeq [l]/{}^{l}K \quad (n-1 \geqq l \geqq 0) \quad (22) $$

If $k_C[X]$ is so large that ${}^{l}k_{\text{eff}} \ll k_C[X]$ for $n \geqq l \geqq 0$ and ${}^{l}k_1 \ll k_C[X]$ for $-1 \geqq l \geqq -m$, it follows from Eqs. (16)—(20) that

$$ I_0/(k_C[X]) \simeq [n] \simeq [n-1] \simeq \cdots \simeq [0] \simeq [-1]_1 \simeq \cdots \simeq [-m+1]_1 \ll [-m]_1 = I_0/{}^{-m}k_1 \quad (23) $$

We are now in a position to discuss fluorescence quantum yields. To the approximation adopted in the present study, it follows from the kinetic analyses given in Paper I that the S_1- and S_2-fluorescence quantum yields obtained on exciting the molecule to the lth level in the absence of the inert gas are

$$ {}^{l}\Phi^0_{1F} = \begin{cases} {}^{l}k_{1F}/{}^{l}k_{\text{eff}} & (n \geqq l \geqq 0) \\ {}^{l}k_{1F}/{}^{l}k_1 & (-1 \geqq l \geqq -m) \end{cases} \quad (24) $$

$$ {}^{l}\Phi^0_{2F} = {}^{l}k_{2F}/({}^{l}K\,{}^{l}k_{\text{eff}}) \quad (n \geqq l \geqq 0) \quad (25) $$

When the molecule is excited to the nth level in the presence of the inert gas, the S_1- and S_2-fluorescence quantum yields, denoted by Φ_{1F} and Φ_{2F} respectively, are given by

$$ \Phi_{1F} = \sum_{l=-m}^{n} {}^{l}k_{1F}[l]_1/I_0 \quad (26) $$

$$ \Phi_{2F} = \sum_{l=0}^{n} \frac{{}^{l}k_{2F}[l]}{{}^{l}KI_0} \quad (27) $$

Here we assume for the sake of simplicity that $k_C[X]$ is negligible in Eq. (10) or (21) compared with ${}^{n}k_{12}$. Strictly speaking, this assumption is not always valid (*cf.* (9)). We can show, however, that even if the above assumption is omitted, the results remain essentially unchanged. Under photostationary conditions the rate of excitation must be equal to the rate of deactivation, so that

$$ I_0 = \sum_{l=0}^{n} {}^{l}k_2[l]_2 + \sum_{l=-m}^{n} {}^{l}k_1[l]_1 $$

Neglecting $k_C[X]$ compared with ${}^{n}k_{12}$ as before, we can rewrite this equation as

$$ I_0 = \sum_{l=0}^{n} {}^{l}k_{\text{eff}}[l] + \sum_{l=-m}^{-1} {}^{l}k_1[l]_1 \quad (28) $$

From Eqs. (24)—(28) and Eq. (20), we obtain

$$ \Phi_{1F} = \frac{\sum_{l=0}^{n} {}^{l}\Phi^0_{1F}\,{}^{l}k_{\text{eff}}[l] + \sum_{l=-m}^{-1} {}^{l}\Phi^0_{1F}\,{}^{l}k_1[l]_1}{\sum_{l=0}^{n} {}^{l}k_{\text{eff}}[l] + \sum_{l=-m}^{-1} {}^{l}k_1[l]_1} \quad (29) $$

$$ \Phi_{2F} = \frac{\sum_{l=0}^{n} {}^{l}\Phi^0_{2F}\,{}^{l}k_{\text{eff}}[l]}{\sum_{l=0}^{n} {}^{l}k_{\text{eff}}[l] + \sum_{l=-m}^{-1} {}^{l}k_1[l]_1} \quad (30) $$

If $k_C[X]$ is large enough for the relation (23) to hold good,[14] we have

$$ \Phi_{1F} \simeq {}^{-m}\Phi^0_{1F} \quad (31) $$

$$ \Phi_{2F} \simeq \sum_{l=0}^{n} {}^{l}\Phi^0_{2F}({}^{l}k_{\text{eff}}/k_C[X]) \quad (32) $$

On the basis of the foregoing kinetic considerations, we examine the spectral data on S_1- and S_2-fluorescence. Referring to Eqs. (29) and (30), we see that Φ_{1F} and Φ_{2F} are closely related to the concentration $[l]$ of the pyrene molecules belonging to the individual levels l. According to Eqs. (16)—(19), as [X] increases, (i) $[l]/[n]$ $(n-1 \geqq l \geqq 0)$ and $[l]_1/[n]$ $(-1 \geqq l \geqq -m)$ increase though $[n]$ itself decreases; and (ii) $[l-1]/[l]$ $(n \geqq l \geqq 1)$,

$[-1]_1/[0]$, and $[l-1]_1/[l]_1$ $(-1 \geqq l \geqq -m+1)$ increase with increasing [X]. The experimental results reported in Paper I indicate that[15]

$$ {}^{n}\Phi_{1F}^{0} < {}^{n-1}\Phi_{1F}^{0} < \cdots < {}^{-m}\Phi_{1F}^{0} \tag{33a} $$

By combining (ii) with (33a), it can be strictly verified that Φ_{1F} given by Eq. (29) possesses its lowest value ${}^{n}\Phi_{1F}^{0}$ at [X]=0, increases with increasing [X], and finally reaches its highest value ${}^{-m}\Phi_{1F}^{0}$ (see Eq. (31)).

On the other hand, the data in Paper I show that

$$ {}^{n}\Phi_{2F}^{0} > {}^{n-1}\Phi_{2F}^{0} > \cdots > {}^{0}\Phi_{2F}^{0} \tag{33b} $$

It follows from (ii) and (33b) that, in contrast to Φ_{1F}, the quantum yield Φ_{2F} given by Eq. (30) decreases with increase in [X]. We note that ${}^{l}\Phi_{2F}^{0}$ falls off markedly with a decrease in the number l (Paper I). On increasing [X] from zero, therefore, Φ_{2F} decreases rapidly from its highest value ${}^{n}\Phi_{2F}^{0}$. At sufficiently large [X], Φ_{2F} is expressed in the form of Eq. (32), and hence it is finally reduced to zero.

These considerations are in good agreement, at least qualitatively, with the results of experiments on the intensities (Fig. 1) and quantum yields (Fig. 3) of the S_1- and S_2-fluorescence.

In order to obtain more quantitative information about the dependence of Φ_{2F} on cyclohexane pressure, we made a calculation on the basis of the stepladder model. We treated a case where the initially excited level n corresponds to $S_4{}^0$. The difference between $E(S_4{}^0)=E(S_2{}^*)$ and $E(S_2{}^0)$ is known to be about 12000 cm^{-1} (Paper I). Referring to the literature,[13] we tentatively adopted two values (500 and 1000 cm^{-1}) as $\Delta\varepsilon$. It then follows that $n=24$ and 12, respectively, for $\Delta\varepsilon=$ 500 and 1000 cm^{-1}. According to Eqs. (16), (25), and (27), Φ_{2F} can be expressed in the form

$$ \Phi_{2F} = \sum_{l=0}^{n} {}^{l}\Phi_{2F}^{0} \frac{{}^{l}k_{eff}}{{}^{n}k_{eff}+k_C[X]} \frac{[l]}{[n]} \tag{34} $$

In Eq. (34), the observed S_2-fluorescence quantum yield as a function of excitation energy (Paper I) was used for ${}^{l}\Phi_{2F}^{0}$. The effective rate constant ${}^{l}k_{eff}$ was assumed to be equal to the reciprocal of the S_1-fluorescence lifetime τ_1 (*vide infra*), which has been measured in the present study as a function of excitation energy (Fig. 4). The rate constant k_C was determined from the standard gas kinetic theory, molecular diameters of 8 and 4 Å being assigned to pyrene and cyclohexane, respectively; the result is $k_C=9.8\times10^6$ $Torr^{-1}$ s^{-1} at 170 °C. The ratio of concentrations, $[l]/[n]$, can be calculated by using Eq. (17) repeatedly. The curves thus obtained theoretically for Φ_{2F} as a function of cyclohexane pressure reproduce fairly well the experimental data, *i.e.*, the lower curve 3 in Fig. 3. The experimental curve lies between the two theoretical ones corresponding to $\Delta\varepsilon=500$ and 1000 cm^{-1}; the latter $\Delta\varepsilon$ value leads to a more favorable result.

The changes in position and shape of the fluorescence spectra on increasing the inert gas pressure must be caused by changes of the extents to which different levels l contribute to the fluorescence transitions concerned.

From Eqs. (16)—(20), (23), and (26) or (29) we may predict that the S_1-fluorescence band will shift toward the position of the emission originating from lower levels, *i.e.* toward the blue, upon increasing the inert gas pressure; and finally, as is seen from Eq. (31), the S_1-fluorescence will originate from the lowest vibrational level of S_1 which gives emission at the shortest wavelengths. The above prediction is in agreement with the behavior of S_1-fluorescence shown in Fig. 1.

The numbers l of the levels responsible for the S_2-fluorescence are such that $n \geqq l \geqq 0$. According to the relations (17) and (23), $[n]>[n-1]>\cdots>[0]$ for any value of [X], and $[n]\simeq[n-1]\simeq\cdots\simeq[0]$ for large [X]. Moreover, as has been mentioned, ${}^{l}\Phi_{2F}^{0}$ decreases rapidly with decreasing l. It then follows from Eq. (27) or (30) that the emissions from the levels with higher l numbers make relatively large contributions to the S_2-fluorescence, irrespective of inert gas pressure. This accounts for the finding that the S_2-fluorescence band shows only small blue shifts even at high inert gas pressures, in contrast to the case where the excitation energy is decreased (Paper II and Fig. 2).

We next proceed to the case of transient processes following the pulse excitation by the breakdown spark. We substitute n for l in both Eqs. (1) and (2), and remove the first terms of the right-hand sides of these equations. In the absence of the inert gas, the fourth terms on the right-hand sides of Eqs. (3) and (4) also are removed. The solution of Eqs. (1) and (2) thus modified is well known.[12] When the relations (5) and (6) hold, $[n]_2$ and $[n]_1$ are expressed in the forms

$$ [n]_2 = [n]_2^0 \left\{ \frac{{}^{n}K}{1+{}^{n}K} \exp(-{}^{n}\tilde{\lambda}_2 t) + \frac{1}{1+{}^{n}K} \exp(-{}^{n}\tilde{\lambda}_1 t) \right\} \tag{35} $$

$$ [n]_1 = [n]_2^0 \frac{{}^{n}K}{1+{}^{n}K} \{ -\exp(-{}^{n}\tilde{\lambda}_2 t) + \exp(-{}^{n}\tilde{\lambda}_1 t) \} \tag{36} $$

where

$$ {}^{n}\tilde{\lambda}_2 = {}^{n}k_{21} + {}^{n}k_{12} \tag{37} $$

$$ {}^{n}\tilde{\lambda}_1 = {}^{n}k_{eff} \equiv 1/{}^{n}\tau_{eff} \tag{38} $$

$[n]_2$ at $t=0$ is written as $[n]_2^0$, while $[n]_1$ is assumed to be zero at $t=0$.

Since ${}^{n}\tilde{\lambda}_2 \gg {}^{n}\tilde{\lambda}_1$, after a very short time, δt, of the order of $1/({}^{n}k_{21}+{}^{n}k_{12})$, $[n]_2$ and $[n]_1$ will decay with a common rate constant, ${}^{n}k_{eff}$. In the range of time longer than δt, it follows from Eqs. (35) and (36) that $[n]_1/[n]_2={}^{n}K$, that is, a sort of dynamic equilibrium is attained.[12] Note that this equation is obtained also by putting [X] $=0$ in Eq. (10).

Because of the duration (~70 ns) of the flash employed, the present experiments on the time behavior of the dual fluorescences must be concerned with the range of time ($>\delta t$) mentioned above. It is thus expected that the observed lifetimes τ_1 and τ_2 are identical and both are equal to ${}^{n}\tau_{eff}$ defined by Eq. (38). Since ${}^{n}K \gg 1$ in Eq. (13). ${}^{n}\tau_{eff}$ is nearly equal to $1/{}^{n}k_1$, which is estimated to be about 10^2 ns and is much longer than the radiative lifetime ($1/{}^{n}k_{2F}$) of S_2, 6 ns from the integrated absorption intensity (Paper I). The lifetime data given in Fig. 4 indicate that τ_2 is, indeed, considerably longer than the radiative lifetime of S_2. In contrast to the results of kinetic considerations, however, τ_2 is slightly shorter than τ_1. This discrepancy in value between the two lifetimes has been interpreted by Deinum *et al.* as due in part to sequence congestion effects.[8]

Suppose now that the pyrene molecule is excited into the level with $l=n$ by a light pulse in the presence of cyclohexane. As the time proceeds, the lower levels $l=n-1$, $n-2$, $\cdots$ are populated owing to the vibrational relaxation caused by the collision, and the fluorescence is emitted also from these levels. On account of the relations (5)—(9), a dynamic equilibrium will be reached in each of the emitting levels. It is then expected from the relations (33a) and (33b) that an increase in cyclohexane pressure will result in a decrease and an increase in decay rate of the S_1- and S_2-fluorescence, respectively. In other words, the apparent lifetime $\bar{\tau}_1$ will be lengthened but $\bar{\tau}_2$ will be shortened, in agreement with the observations illustrated in Fig. 5.

Effects of Oxygen. When oxygen is added to the pyrene vapor, the S_1- and S_2-fluorescence emissions are quenched, but their spectral shapes and positions are little changed (see Figs. 6 and 7), suggesting that the vibrational relaxation is not induced by collision with oxygen. We are therefore concerned here solely with the vibronic level S_2*, which is initially excited (directly or indirectly), and its isoenergetic partner S_1*. The rate equations and related quantities that have hitherto been used for the vibrational level, $l=n$, can be applied to the case of oxygen quenching by making pertinent modifications. The superscript n will hereafter be eliminated.

The oxygen-quenching rate of the vibronic state S_i* may be expressed in the form $wk_Q[Y][S_i^*]$, where [Y] is the concentration of the quencher Y, *i.e.* oxygen, and w is a factor representing the probability that one collision quenches S_i*. In the present study the following relations hold: $k_{21} \gg wk_Q[Y]$ and $k_{12} \gg wk_Q[Y]$ or $k_{12} \gtrsim wk_Q[Y]$ (*cf.* relations (8) and (9)). Thus, under photostationary conditions, it follows from Eqs. (16), (20), and (21) that

$$\Phi_{1F} = k_{1F}/(k_{eff}+wk_Q[Y]) \tag{39}$$

$$\Phi_{2F} = \frac{k_{2F}}{k_{eff}+wk_Q[Y]} \frac{1+wk_Q[Y]/k_{12}}{K} \tag{40}$$

where K and k_{eff} are defined by Eqs. (12) and (13). The quantum yields in the absence and the presence of Y will be denoted, respectively, by Φ_{iF}^0 and Φ_{iF}. Then Eqs. (39) and (40) lead to the following equations of the Stern-Volmer type:

$$\Phi_{1F}^0/\Phi_{1F} = 1 + wk_Q\tau_{eff}[Y] \tag{41}$$

$$\frac{\Phi_{2F}^0}{\Phi_{2F}} = \frac{1+wk_Q\tau_{eff}[Y]}{1+wk_Q[Y]/k_{12}} \tag{42}$$

with $\tau_{eff}=1/k_{eff}$. Unless $wk_Q[Y]$ is of comparable magnitude to k_{12}, the denominator on the right-hand side of Eq. (42) may be equated to unity.

The Stern-Volmer plots shown in Fig. 8 are in general agreement with the prediction from Eqs. (41) and (42), except that two straight lines resulting from the plots of the quantum yield ratios Φ_{1F}^0/Φ_{1F} and Φ_{2F}^0/Φ_{2F} which were measured with the same excitation energy have somewhat different slopes. Such a difference between the slopes may be attributed to the fact that the observed lifetimes τ_1 and τ_2, which are both identified as τ_{eff}, are not strictly equal to each other, as has already been mentioned.

Table 1. Kinetic data on quenching of S_1- and S_2-fluorescence by oxygen

Fluorescing state	Exciting wavelength (nm)	Slope of Stern-Volmer plot (Torr^{-1})	Lifetime τ_1 or τ_2 (ns)	$wk_Q\times10^{-11}$ (1 mol^{-1}. s^{-1})	w
S_1	324 (S_2^0)	1.14	157	2.00	0.77
	298 (S_2^2)	0.93	116	2.20	0.85
	266 (S_3^0)	0.71	92	2.14	0.82
	257 (S_3^1)	0.66	81	2.26	0.87
	234 (S_4^0)	0.39	54	1.98	0.75
	226 (S_4^1)	0.36	52	1.93	0.74
S_2	298 (S_2^2)	0.54	—	—	—
	266 (S_3^0)	0.43	65	1.83	0.71
	257 (S_3^1)	0.40	—	—	—
	234 (S_4^0)	0.30	45	1.84	0.71
	226 (S_4^1)	0.24	—	—	—

The values for the quenching rate constant wk_Q, obtained at various exciting wavelengths, are listed in Table 1, together with the slopes and lifetimes from which the wk_Q values were derived. In contrast to the considerable variation of the lifetimes with exciting wavelength, both S_1- and S_2-fluorescence emissions show comparatively constant wk_Q values, ranging from 1.8×10^{11} to 2.3×10^{11} 1 mol^{-1} s^{-1}, regardless of the excitation energy. Assuming molecular diameters to be 8 and 2 Å for pyrene and oxygen, respectively, we obtain $k_Q=2.6\times10^{11}$ 1 mol^{-1} s^{-1} (or 9.4×10^6 Torr^{-1} s^{-1}) at 170 °C from the gas kinetic theory. Dividing the experimental wk_Q value by the theoretical k_Q, we get the probability factor w. The w values thus determined are found to be rather close to unity (Table 1). Although some assumptions are involved in the evaluation of w, it may be concluded that the quenching of the dual fluorescences of pyrene vapor by oxygen is very efficient.

Inspection of the data in Table 1 at exciting wavelengths of 234 and 266 nm reveals that the difference in question between the slopes of the Stern-Volmer plots is due mainly to the difference between τ_1 and τ_2. For a given exciting wavelength, the S_2-fluorescence has a small slope compared with the S_1-fluorescence, so that the intensity of the S_2-fluorescence spectrum relative to that of the S_1-fluorescence increases with the oxygen pressure. As a result, the S_2-fluorescence spectrum becomes more distinct at higher oxygen pressures (see Figs. 6 and 7). In the case of spectral curve 3 in Fig. 6 (S_2^2 excitation at 350-Torr oxygen pressure), the S_2-fluorescence can be observed very clearly, and its intensity relative to the intensity of the S_1-fluorescence is somewhat higher than expected from extrapolation of the linear plots shown in Fig. 8. A conceivable reason for the occurrence of this phenomenon is that in the case concerned the denominator on the right-hand side of Eq. (42) is appreciably larger than unity.

Relations between Rate Constants. In Paper I we attempted to determine the values of the rate constants k_{21} and k_{12}. For that purpose the S_2-fluorescence quantum yield Φ_{2F} was divided into two parts, that is, $\Phi_{2F}=\phi_{2F}+\phi_{12F}$, where ϕ_{2F} and ϕ_{12F} correspond to the quantum yields of the prompt and slow fluorescence

emissions, respectively. The ratio of ϕ_{12F} to ϕ_{2F} was then expressed as

$$\phi_{12F}/\phi_{2F} = \Phi_{1F}(k_{12}/k_{1F}) \quad (43)$$

On the assumption that the residue of S_2-fluorescence at a high pressure of cyclohexane (~70 Torr) ocrresponds to ϕ_{2F}, the ratio ϕ_{12F}/ϕ_{2F} was estimated to be 25 for S_4^0 excitation. As is seen in Fig. 3, Φ_{2F} is still decreasing at a cyclohexane pressure of 70 Torr. Furthermore, the contribution of thermal repopulation to Φ_{2F} (Paper I) cannot be ignored at high cyclohexane pressures. The figure 25 for ϕ_{12F}/ϕ_{2F}, therefore, should be regarded as a tentative one.

As has been mentioned, oxygen quenches the S_1 and S_2 states of pyrene very efficiently, so that practically no vibrational relaxation takes place even at oxygen pressures higher than 100 Torr. Hence, it is not necessary to take account of the thermal repopulation effect when oxygen is used as a foreign gas. So far as the Stern-Volmer plot based on Eq. (42) is linear, the prompt fluorescence yield, ϕ_{2F}, should be negligible compared with ϕ_{12F}. On the basis of these considerations, we inferred from such experimental data as shown in Figs. 6—8 that $\phi_{12F}/\phi_{2F} \gtrsim 10^2$ irrespective of excitation wavelength. It then follows from Eq. (43) that $k_{12} \gtrsim 10^9\ s^{-1}$, since k_{1F} is $10^6\ s^{-1}$ (Paper I). On the other hand, according to Paper I,

$$k_{21} \simeq k_{12}\frac{\Phi_{1F}}{\Phi_{2F}}\frac{k_{2F}}{k_{1F}} \quad (44)$$

Φ_{1F}/Φ_{2F} is ~10 for S_4^0 excitation and increases with decreasing excitation energy, and k_{2F} is known to be $1.7\times10^8\ s^{-1}$ (Paper I); hence $k_{21} > 10^{12}\ s^{-1}$. Thus, it may safely be said that the relations (5)—(7) hold at excitation wavelengths adopted in the present study.

Concluding Remarks. In this paper we hold the view that electronic processes in an isolated pyrene molecule may be treated kinetically on the basis of a scheme in which internal conversion is reversible between S_1* and S_2*, and thereby we can explain, to a good extent, the effects of cyclohexane and oxygen on the dual fluorescences of pyrene vapor. Along this line, it is concluded from the results of the present study that the S_2-fluorescence consists mainly of a slow component originating from S_2* which is in equilibrium with S_1*.

Quantum-mechanically, an intermediate strong coupling[8,16] is expected to occur between S_2* and S_1* because of a small electronic energy gap (3900 cm^{-1}) between the S_2 and S_1 states of the pyrene molecule. The coupling of an S_2* vibronic state with S_1* states that are quasidegenerate with S_2* yields compound states, and results in an anomalously long lifetime of the S_2-fluorescence. Thus, a good correspondence between the kinetic and quantum-mechanical schemes is obtained, as has recently been pointed out by Lahmani *et al.*[2]

Although it is predicted from each of the two schemes that the lifetimes τ_1 and τ_2 for the S_1- and S_2-fluorescence emissions should be equal, there is a slight but systematic difference between the actually obtained values of τ_1 and τ_2. Owing to sequence congestion, the thermal distribution of vibrational energy in the electronic ground state is transferred to the excited state even if a molecular system is excited with light of a given energy. According to Deinum *et al.*[8] the sequence congestion, along with the rapid increase of Φ_{2F}/Φ_{1F} with the excess vibrational energy, may account for about half of the lifetime difference. Further studies must be made to settle this problem.

We wish to express our thanks to Mr. Yoshio Shindo, Mr. Masahisa Fujita, and Mr. Masakatsu Aoi for their help in carrying out the experiments.

References

1) B. R. Henry and W. Siebrand, "Organic Molecular Photophysics," Vol. 1, ed. by J. B. Birks, John Wiley & Sons, London (1973), Chap. 4.
2) F. Lahmani, A. Tramer, and C. Tric, *J. Chem. Phys.*, **60**, 4431 (1974).
3) A. Frad, F. Lahmani, A. Tramer, and C. Tric, *ibid.*, **60**, 4419 (1974).
4) Papers cited in Refs. 2) and 3).
5) H. Baba, A. Nakajima, M. Aoi, and K. Chihara, *J. Chem. Phys.*, **55**, 2433 (1971).
6) H. Baba and M. Aoi, *J. Mol. Spectrosc.*, **46**, 214 (1973).
7) P. A. Geldof, R. P. H. Rettschnick, and G. J. Hoytink, *Chem. Phys. Lett.*, **4**, 59 (1969).
8) T. Deinum, C. J. Werkhoven, J. Langelaar, R. P. H. Rettschnick, and J. D. W. van Voorst, *ibid.*, **27**, 206, 552 (1974).
9) P. Wannier, P. M. Rentzepis, and J. Jortner, *ibid.*, **10**, 102 (1971).
10) T. Brewer, *J. Amer. Chem. Soc.*, **93**, 775 (1971).
11) J. E. Haebig, *J. Phys. Chem.*, **71**, 4203 (1967).
12) J. B. Birks, "Photophysics of Aromatic Molecules," Wiley-Interscience, London (1970).
13) a) M. Boudart and J. T. Dubois, *J. Chem. Phys.*, **23**, 223 (1955); b) A. M. Halpern and W. R. Ware, *ibid.*, **53**, 1969 (1970); c) B. S. Rabinovitch, H. F. Carroll, J. D. Rynbrandt, J. H. Georgakakos, B. A. Thrush, and R. Atkinson, *J. Phys. Chem.*, **75**, 3376 (1971).
14) In this case, it follows from the simplest stepladder model being adopted here that vibrational levels other than S_1^0 are little populated. In reality the lower vibrational levels are to be populated according to Boltzmann's distribution.
15) See also C. J. Werkhoven, T. Deinum, J. Langelaar, R. P. H. Rettschnick, and J. D. W. van Voorst, *Chem. Phys. Lett.*, **32**, 328 (1975).
16) A. Nitzan, J. Jortner, and P. M. Rentzepis, *Proc. Roy. Soc. Ser. A*, **327**, 367 (1972).